Soft X-Ray Measurement on the Collisional Merging Process in a Field-Reversed Configuration[*)]

Junichi SEKIGUCHI, Tomohiko ASAI and Tsutomu TAKAHASHI

College of Science and Technology, Nihon University, Tokyo 101-8308, Japan

(Received 10 January 2019 / Accepted 7 May 2019)

To investigate excited shockwaves in a collisional-merging field-reversed configuration (FRC), soft X-ray (SXR) measurement was initiated on the FRC amplification via translation collisional merging (FAT-CM) instrument. Since the FRCs collide at a relative speed of 300 - 400 km/s on the FAT-CM, which is faster than the Alfvén velocity in the separatrix, shockwaves are assumed to be excited in the colliding FRCs. These excited shockwaves would play an important role in energy conversion during the collisional merging formation process of the FRC. The relation between the global behavior of the FRC in the collisional merging process and the time evolution of SXR signals are discussed herein.

Keywords: field-reversed configuration, shockwave, collisional merging, super-Alfvénic translation

DOI: 10.1585/pfr.14.3402116

1. Introduction

Compact torus (CT), such as field-reversed configuration (FRC) and spheromaks, have toroidal magnetic configuration with simply-connected geometry [1]. A CT can be accelerated by a magnetic pressure gradient and translated axially. This translation technique provides the separation of the formation and burning sections in the reactor in order to fuel the reactor core plasma and perform merging of the CTs. Spheromak-merging experiments [2] show the energy conversion in which the magnetic energy of spheromaks is converted into the thermal energy of a merged FRC thorough magnetic reconnection. Collisional merging of two FRCs at super-Alfvén velocity was performed on the C-2/C-2U device [3]. In the collisional merging experiments, axial kinetic energy is converted mostly into thermal ion energy of the merged FRC plasma. Although FRC by collisional merging formation shows significantly higher performance compared with single-translated FRC, the details of the collisional merging process are unclear.

In order to investigate the collisional merging process of FRC at super-Alfvén velocity, the FRC amplification via translation (FAT) device was recently upgraded to a FAT collisional merging (FAT-CM) [4]. In this work, since the FRCs collide at a relative axial velocity of 300 - 400 km/s, which is faster than the Alfvén velocity in the separatrix, shockwaves are assumed to be excited in the colliding FRCs. Excited shockwaves would play an important role in the energy conversion during the collisional merging formation process of FRC [5]. Shock-based heating is the most effective mechanism in plasmas, with most ions in the field-reversed theta-pinch (FRTP) formation process [1]. In the FRC translation experiment on the FRC Injection Experiment (FIX), FRC plasma translated into mirror magnetic field at super-Alfvén speed was re-thermalized by collision-less shockwaves [6]. A similar heating process could occur in the collisional merging process on the FAT-CM. To investigate the excited shockwaves in the colliding FRCs, soft X-ray (SXR) measurement was attempted on the FAT-CM. The relation between the global behavior of the FRC in the collisional merging process and the time evolution of the SXR signal are discussed.

2. Experimental Device

Figure 1 shows a schematic diagram of the FAT-CM device. The device comprises two FRTP formation sections as FRC sources and a central confinement vessel to perform collisional merging. The formation sections are called "R-formation" and "V-formation," respectively. Deuterium gas is introduced via gas-puff valves mounted at the ends of both formation sections. Quasi-static magnetic confinement field coils are placed along the confinement section. Details of the FAT-CM parameter and basic diagnostic are described in the reference of [4].

Figure 2 shows a schematic diagram of the SXR measurement, with three beryllium film filters installed at the midplane of the confinement vessel. A negatively biased voltage of 45 V was applied to a silicon surface barrier detector (ORTEC, BU-012-50-100) [7] with an affective area of 50 mm^2, by a battery. Visible light was blocked using a beryllium film of ϕ18 mm. Thus, bremsstrahlung radiation in the range of SXR from the plasma is detected [8]. Since two of the beryllium films are retractable, the total thick-

author's e-mail: sekiguchi.junichi@nihon-u.ac.jp

*) This article is based on the presentation at the 27th International Toki Conference (ITC27) & the 13th Asia Pacific Plasma Theory Conference (APPTC2018).

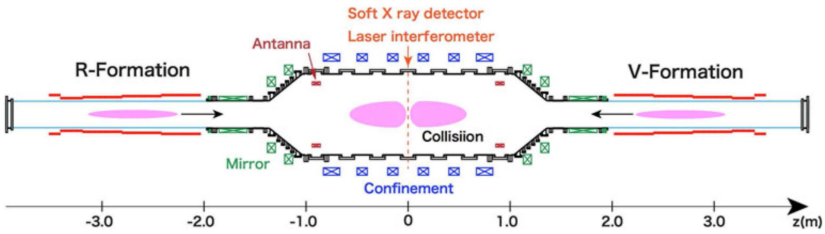

Fig. 1 Schematic diagram of the experimental device FAT-CM.

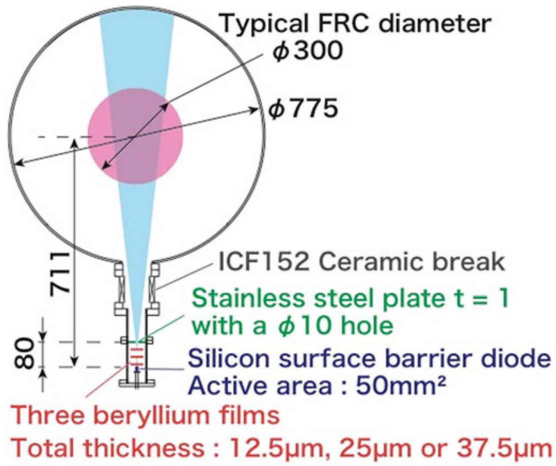

Fig. 2 Schematic diagram of the SXR measurement.

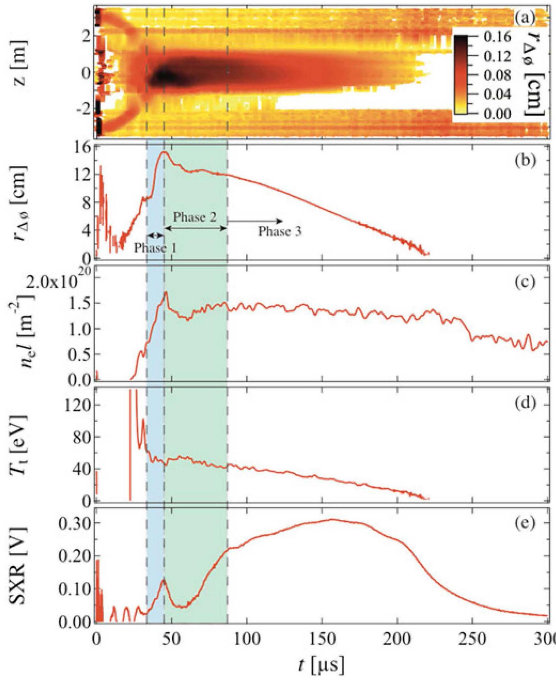

Fig. 3 Time evolutions of (a) the contour of excluded flux radius, (b) the excluded flux radius, (c) the double-passed, line-integrated electron density, (d) the total temperature and (e) the SXR signal for a typical merged FRC (#11049).

ness can be switched to 12.5, 25, or 37.5 μm. To limit the field of view, indicated by light blue in Fig. 3, a stainless-steel disk (SS304, 1-mm thick) with a ϕ10-mm hole was mounted. The thickness of the beryllium film was fixed at 37.5 μm in the present work.

3. Experimental Results

Figure 3 shows the time evolutions of the excluded flux radius, the double-passed, line-integrated electron density, the total temperature, and the output signal of the SXR detector measured at the midplane of the confinement section. In this series of experiments, two individually formed FRCs, whose radius, length, electron density, and total plasmoid temperature are about 5 cm, 0.6 m, 2×10^{21} m^{-3}, and 110 eV, respectively, and collide around the midplane at a relative axial velocity of 300 - 400 km/s. The FRC expands in volume in the collisional merging process and settles into an equilibrium state.

The three phases of the collisional merging process are defined as shown in Fig. 3. In phase 1, the volume of the plasmoid rapidly increases mainly due to radial expansion. The length of the plasmoid ranges from 1.5 - 2.0 m during the collision, merging and equilibrium phases. The line-integrated electron density and the SXR signal also increase during phase 1. The SXR signal amplitude can be assumed to be $T_e^{0.5} n_e^2 \int \exp\{-E/T_e\} T(E) dE$, where $T(E)$ is the transmission function determined by the metallic filter and the absorption function of the detector [9, 10]. The peak of the excluded flux radius profile is flattened in the phase 2. The SXR signal transits to a modestly increasing phase, defined as phase 3. Here, T_t is calculated from the pressure balance as

$$T_t = T_e + T_i = \langle\beta\rangle B_e^2 / 2\mu_0 k_B \langle n_e \rangle, \quad (1)$$

$$\langle\beta\rangle = 1 - 0.5(r_{\Delta\phi}/r_t)^2, \quad (2)$$

where $\langle\beta\rangle$, B_e, μ_0, k_B, $\langle n_e \rangle$ and r_t are the average beta, external magnetic flux density, permeability, Boltzmann constant, average electron density and wall radius, respectively.

Figure 4 shows ΔB (= $B_p - B_v$), which is the difference of the external magnetic field with and without the colliding plasmas, measured by an array of pick-up coils installed on the inside-wall of the confinement vessel. The ΔB corresponds to the excluded flux $\Delta\phi = (r_{\Delta\phi}/r_t)^2 B_p$. The relative velocity of the colliding FRCs is estimated

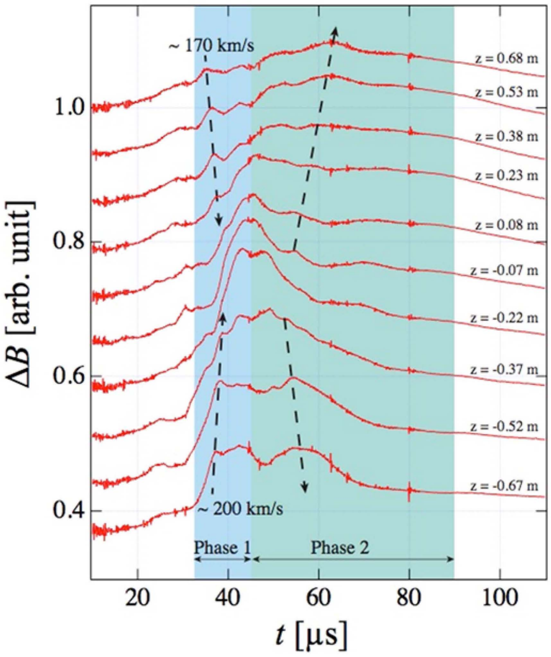

Fig. 4 Time evolution of the external magnetic field on the collisional merging process (#11049).

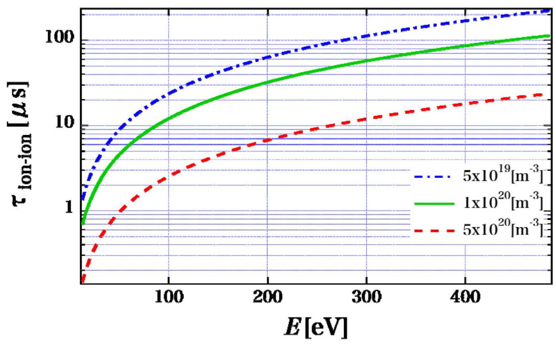

(a) Ion-ion collision time

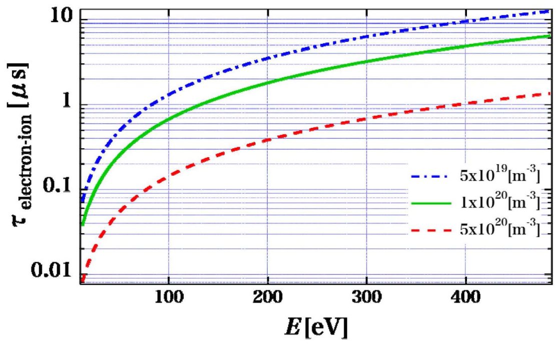

(b) Electron-ion collision time

Fig. 5 Collision time calculated by the FAT-FRC plasma parameters.

as 370 km/s using the time-of-flight method with the magnetic field, and is indicated by dashed lines in Fig. 4 in phase 1. The Alfvén velocity in the FAT-FRC is roughly 80 km/s, calculated from the experimentally measured line-integrated electron density and the external magnetic field. Although this Alfvén velocity is not estimated locally, the Alfvén Mach number would be greater than 4 in the separatrix, because the internal magnetic field of the FRC generally shows a trend to decrease toward a magnetic axis. A significant hump in the excluded flux, which is probably caused as the result of generated shockwaves, is observed around the midplane of the confinement vessel [11]. The dashed lines after the collision in phase 2 indicate a propagating hump in the excluded flux radius. The hump occurs due to increased pressure via the process of re-thermalization of ion kinetic energy into thermal energy.

4. Discussion

The thermal relaxation time is evaluated to compare the time evolution of the SXR signal. Ion-ion and electron-ion collision time for the formed FRC plasma parameters are calculated as shown in Fig. 5. The ion-ion collision time in the FRC is about 10 µs, which is comparable to the duration of phase 2 in Fig. 3. The electron-ion collision time is shorter than the time scale of the global motion in the collisional merging process. This indicates that the axial ion momentum is thermalized by the ion-ion thermal equilibrium in phase 2. Then the electrons in the merged FRC are heated by ion-electron collision until reaching thermal equilibrium. In phase 3, the total temperature decreases but the SXR signal amplitude increases. This is because ion-electron thermal relaxation time is faster than the time scale of decreasing T_t. The time evolution of the ion or electron temperature up to thermal equilibrium is shown as below [12]:

$$T_t = T_e + T_i : (T_i > T_e), \tag{3}$$

$$\frac{dT_e}{dt} = \frac{1}{\tau_{eq}}(T_i - T_e), \tag{4}$$

where τ_{eq} is the energy equilibration time between ions and electrons. Although the ratio of ion temperature and electron temperature is not estimated, ion temperature would be much higher than electron temperature given the shock heating.

The transition of the internal magnetic field profile in the collisional merging process was experimentally observed on the FAT-CM [13]. The internal magnetic field profile was experimentally observed by an array of pick-up coils installed at the midplane where the SXR detector is mounted. The SXR and internal magnetic field profiles were not measured at the same time because the field of view was intercepted by the array. The internal magnetic field structures in phase 1 (at 46 µs), and in phase 2 (at 80 µs), have a clear, field-reversed structure. At phase 1, a strong B_t field is observed. The local toroidal magnetic field component could be measured by a shift or tilt motion of the FRC containing no toroidal magnetic flux [14]. Moreover, toroidal magnetic flux can be generated by the

FRC translation process [15]. The observed B_t field profile evolution and the change in direction indicate a plasma motion/shift in axial direction. In phase 2 (at 80 μs), there remains a modest B_t field without changing of positive and negative signs. The reversed B_p field in phase 2 shows good agreement with the rigid rotor profile model [1], which is commonly used to model the poloidal flux structure during the equilibrium phase. The time scale of the transition of the internal magnetic field profile is also comparable to the risetime of the SXR signal.

5. Summary

The newly installed SXR measurement on the FAT-CM showed a relation between SXR intensity and global motion during and after the collisional merging process of two FRCs. The axial ion momentum is likely to be thermalized by the ion-ion equilibrium once the calculated ion-ion collision time is comparable to the duration of the risetime of the SXR intensity.

Acknowledgement

This work was supported in part by a Grant-in Aid for Scientific Research JP16K06939 from the Japan Society for the Promotion of Science (JSPS).

[1] M. Tuszewski, Nucl. Fusion **28**, 2033 (1988).
[2] Y. Ono, M. Inomoto, Y. Ueda, T. Matsuyama and T. Okazaki, Nucl. Fusion **39**, 2001 (1999).
[3] Y. Guo, M.W. Binderbauer, D. Barnes, S. Putvinski, N. Rostoker, L. Sevier, M. Tuszewski, M.G. Anderson, R. Andow, L. Bonelli, F. Brandi, R. Brown, D.Q. Bui, V. Bystritskii, F. Ceccherini, R. Clary, A.H. Cheung, K.D. Conroy, B.H. Deng, S.A. Dettrick, J.D. Douglass, P. Feng, L. Galeotti, E. Garate, F. Giammanco, F.J. Glass, O. Gornostaeva, H. Gota, D. Gupta, S. Gupta, J.S. Kinley, K. Knapp, S. Korepanov, M. Hollins, I. Isakov, V.A. Jose, X.L. Li, Y. Luo, P. Marsili, R. Mendoza, M. Meekins, Y. Mok, A. Necas, E. Paganini, F. Pegoraro, R. Pousa-Hijos, S. Primavera, E. Ruskov, A. Qerushi, L. Schmitz, J. H. Schroeder, A. Sibley, A. Smirnov, Y. Song, L.C. Steinhauer, X. Sun, M.C. Thompson, A.D. Van Drie, J.K. Walters and M.D. Wyman, Phys. Plasmas **18**, 056110 (2011).
[4] T. Asai, A. Hosozawa, D. Kobayashi, H. Gota, J. Sekiguchi, J. Ishiwata, M. Inomoto, M.W. Binderbauer, N. Ono, S. Dettrick, S. Okada, T. Roche, T. Tajima, To. Takahashi, Ts. Takahashi and Y. Mok, in 27th IAEA-FEC 2018, Gandhinagar, India (2018) EX/P7-20.
[5] M.W. Binderbauer, T. Tajima, L.C. Steinhauer, E. Garate, M. Tuszewski, L. Schmitz, H.Y. Guo, A. Smirnov, H. Gota, D. Barnes, B.H. Deng, M.C. Thompson, E. Trask, X. Yang, S. Putvinski, N. Rostoker, R. Andow, S. Aefsky, N. Bolte, D.Q. Bui, F. Ceccherini, R. Clary, A.H. Cheung, K.D. Conroy, S.A. Dettrick, J.D. Douglass, P. Feng, L. Galeotti, F. Giammanco, E. Granstedt, D. Gupta, S. Gupta, A.A. Ivanov, J.S. Kinley, K. Knapp, S. Korepanov, M. Hollins, R. Magee, R. Mendoza, Y. Mok, A. Necas, S. Primavera, M. Onofri, D. Osin, N. Rath, T. Roche, J. Romero, J.H. Schroeder, L. Sevier, A. Sibley, Y. Song, A.D. Van Drie, J.K. Walters, W. Waggoner, P. Yushmanov, K. Zhai and TAE Team, Phys. Plasmas **22**, 056110 (2015).
[6] H. Himura, S. Ueoka, M. Hase, R. Yoshida, S. Okada and S. Goto, Phys. Plasmas **5**, 4262 (1998).
[7] K.W. Wernzel and R.D. Petrasso, Rev. Sci. Instrum. **59**, 1380 (1988).
[8] F.C. Jahoda, E.M. Little, W.E. Quinn, G.A. Sawyer and T.F. Stratton, Phys. Rev. **119**, 843 (1960) or J. Kiraly, M. Bitter, P. Eftimion, S. Von Goeler, B. Grek, K.W. Hill, D. Johnson, K. McGuire, N. Sauthoff, S. Sesnic, F. Stauffer, G. Tait and G. Taylor, Nucl. Fusion **27**, 397 (1987).
[9] J. Kiraly, M. Bitter, S. von Goeler, K.W. Hill, L.C. Johnson, K. McGuire, S. Sesnic, N.R. Sauthoff, F. Tenney and K.M. Young, Rev. Sci. Instrum. **56**, 827 (1985).
[10] L. Delgado-Aparicio, K. Tritz, T. Kramer, D. Stutman, M. Finkenthal, K. Hill and M. Bitter, Rev. Sci. Instrum. **81**, 10E303 (2010).
[11] H.A.B. Bodin, T.S. Green, G.B.F. Niblett, N.J. Peacock, J.M.P. Quinn, J.A. Reynolds and J.B. Taylor, Nucl. Fusion Supplement **2**, 511 (1962).
[12] D.J. Rej, G.A. Barnes, M.H. Baron, R.E. Chrien, S. Okada, R.E. Siemon, D.P. Taggart, M. Tuszewski, R.B. Webster and B.L. Wright, Nucl. Fusion **30**, 6 (1990).
[13] H. Gota, J. Ishiwata, F. Tanaka, A. Hosozawa, T. Asai, Ts. Takahashi, J. Sekiguchi, T. Roche, T. Matsumoto, S. Dettrick, Y. Mok, M.W. Binderbauer and T. Tajima, Rev. Sci. Instrum. **89**, 10J114 (2018).
[14] T. Ikeyama, M. Hiroi, Y. Nemoto and Y. Nogi, Rev. Sci. Instrum. **79**, 063501 (2008).
[15] R.D. Milroy and J.U. Brackbill, Phys. Fluids **29**, 1184 (1986).